Brownian Dynamics Study of a Multiply-Occupied Cation Channel: Application to Understanding Permeation in Potassium Channels

Sam Bek* and Eric Jakobsson‡

*Graduate Program in Biology and ‡Department of Physiology and Biophysics, National Center for Supercomputing Applications, University of Illinois, Urbana, Illinois 61801 USA

ABSTRACT The behavior of a multiply-occupied cation-selective channel has been computed by Brownian dynamics. The length, cross-section, ion-ion repulsion force, and ionic mobility within the channel are all estimated from data and physical reasoning. The only free parameter is a partition energy at the mouth of the channel, defining the free energy of an ion in the channel compared to the bath. It is presumed that this partition energy is associated with the energetics of exchanging a bulk hydration environment for a channel hydration environment. Varying the partition energy alone, keeping all other parameters fixed, gives approximately the full range of magnitudes of single channel conductances seen experimentally for K channels. Setting the partition energy at −11 kT makes the computed channel look similar to a squid axon K channel with respect to magnitude of conductance, shape of the I-V curve, non-unity of Ussing flux ratio exponents, decrease of current and increase of conductance with extracellular ion accumulation, and saturation at high ion concentration in the bathing solution. The model includes no preferred binding sites (local free energy minima) for ions in the channel. Therefore it follows that none of the above-mentioned properties of K channels are strong evidence for the existence of such sites. The model does not show supersaturation of current at very high bathing concentrations nor any pronounced voltage-dependence of the Ussing flux ratio exponent, suggesting that these features would require additional details not included in the model presented herein.

INTRODUCTION

Based on flux measurements of radiotracers, it has been known for many years that some ion channels are multiply occupied by permeant species (Hodgkin and Keynes, 1955). Thus the independence principle, which is implicit in the Goldman-Hodgkin-Katz electrodiffusion equation (Goldman, 1943), is not expected to be valid for a detailed description of such channels. It is formally possible to take ion-ion interactions into account in an analytical theory for ion movement in the channel that combines the Nernst-Planck electrodiffusion equation with the Poisson equation (deLevie et al, 1972; Cooper et al., 1985; Levitt, 1991a,b; Chen and Eisenberg, 1993). However, the mathematics of these analytical Nernst-Planck-Poisson (NPP) theories is quite difficult. Partly because of this difficulty, Eyring or transition-state theories were introduced to describe ion motion in multiply-occupied channels (Hille and Schwarz, 1978). This type of theory reduces a complicated electrodiffusion equation to a problem in linear algebra. (For a review of this theory and its consequences, see Hille, 1992.) Unfortunately, it now seems unlikely that the underlying low-friction physical assumptions of transition state theory will pertain to the interior of actual ion channels, so that diffusion theory is more physically correct (Chiu et al., 1993).

Received for publication 15 September 1993 and in final form 13 January 1994.

Address reprint requests to Eric Jakobsson, Department of Physiology and Biophysics, 5600 Beckman Institute for Advanced Science and Technology, Drawer 25, University of Illinois, 405 North Mathews Avenue, Urbana, IL 61801. Tel.: 217 244 0072; Fax: 217 244 2909; E-mail: jake@silibio.ncsa.uiuc.edu.

0006-3495/94/04/1028/11 $2.00

A straightforward way of solving diffusion problems that include complicated boundary conditions or multiparticle interactions is via Brownian dynamics (Cooper et al., 1985; Davis et al., 1991). This method exploits the underlying identity between diffusion and a random walk (Einstein, 1926). Because of this identity, solution of an electrodiffusion problem by Brownian dynamics should give the same answer as analytical theory, with the caveat that the Brownian dynamics solution will have some noise. This correspondence between Brownian dynamics and analytical theory was demonstrated by Cooper et al. (1985) for the case of the constant-field theory and by Jakobsson and Chiu (1987) for the electrodiffusion theory of the singly-occupied channel (Levitt, 1986). In both of these cases there is no ion-ion interaction in the channel. Cooper et al. (1985) also compared Brownian dynamics with the NPP results of deLevie et al. (1972) for ions interacting in, and permeating, a membrane. In this case the results from the two methods did not agree. The problem was that the NPP theory overestimated the ion-ion repulsive interactions. Because the NPP theory included all the time-averaged permeant ion charge in the membrane in calculating electrostatic repulsions, there was an implicit contribution from ions interacting with themselves. This self-interaction contribution is nonphysical. It is automatically excluded in any Brownian dynamics computation and in any explicitly particulate electrostatic computation and is negligible in a continuum calculation for a space that is large enough to contain many charged particles. In an ion channel, however, there are never more than a few ions at a time, so the NPP theory significantly overestimates the ion-ion repulsion by failing to subtract the nonphysical self-interaction contribution.

The present paper uses Brownian dynamics to explore the properties that arise from ion-ion repulsive interactions in a selective ion channel in which more than one ion of the same

species may reside simultaneously. The results are specifically related to experimental results seen in K channels. (For a recent review of K channel phenomenology, see Pallotta and Wagoner, 1992.)

METHODS AND DETAILS OF MODEL

The methods of the Brownian dynamics simulations are essentially identical to those described by Cooper et al. (1985). In each time step, each ion in the system is moved a random distance based on a random number chosen from a pool with a Gaussian distribution according to the following equation:

$$\Delta x = -(D/RT)(dU/dx)\Delta t + \mathrm{GRN} \times (2D\Delta t)^{1/2} \quad (1)$$

where Δx is the distance that an ion moves in the time interval Δt,

D is the diffusion coefficient,
R is the gas constant,
T is the absolute temperature,
dU/dx is the free energy gradient.

GRN is a random number chosen from a Gaussian distribution such that the mean = 0 and the mean of the squares = 1.

The electrostatic component of the free energy gradient, dU/dx, is $zF(dV/dx)$, where z is the valence of the ion, F is Faraday's constant, and dV/dx is the voltage gradient. The voltage gradient comes from the applied transmembrane voltage plus the field due to other ions in the channel. In addition to the electrostatic component, the free energy gradient within 2 Å of the channel mouth has a component associated with the partitioning of the ions into the channel (Fig. 1 *A*). This partition energy is just the free-energy difference between having the ion solvated by water in the bulk solution as opposed to having it in whatever water and channel solvation domain exists in the channel lumen. There is no precise significance to the 2 Å transition distance. It is somewhat less than the diameter of a potassium ion, so it is an approximately correct level of granularity in defining when an ion is in or out of the channel. For the simulations shown in this article, the diffusion coefficient for the ions in the channel was 1.98×10^{-5} cm^2/s, which is the same as for potassium ions in bulk solution (Hille, 1992). The time step was 1 ps. This time step and mobility leads to a mean thermal jump distance of 0.67 Å per time step. In cases where a single time step carried the ion into or out of the 2 Å transition region at the mouth, the program calculated the fraction of the time step that the ion was in the transition region. Then the trajectory in that time step was recalculated using a new force, namely the force in the transition region times the fraction of the time step that the particle was in the region. To calculate the ion-ion repulsion in the channel, Coulombic repulsion with a dielectric constant of 20 was used for all of the simulations whose results are shown. There is no firm basis for this choice, but it should be near accurate. The reasoning is that the ion-ion repulsion should be less than in the lipid (dielectric constant = 2) because the interior of the channel is aqueous, but greater than in the bulk solution (dielectric constant = 80) because of the surrounding lipid. 20 is intermediate between 2 and 80. To test the sensitivity of the calculations to the intensity of the ion-ion force, the simulations of Fig. 2 were done with dielectric coefficients of 5 and 40, as well as 20. The qualitative behaviors of the system were unchanged. The quantitative effects will be described in the Discussion and Summary section of this paper. Any detailed calculation of the ion-ion repulsion would need to calculate the image potentials associated with the charges at the boundaries of the regions with different dielectric constants (Jordan, 1982). This calculation would be demanding and would have substantial uncertainties due to lack of taking into account a detailed channel structure, which is not known for any biological channel. Thus it was decided that not enough accuracy would be gained in a more precise calculation to warrant the effort. Rather it was deemed appropriate to utilize the shorthand of using the intermediate dielectric constant for the ion-ion repulsion. The algorithm for the ion-ion force was as follows: In each time step, an initial trajectory was calculated based on the ion-ion repulsion at the beginning of the time step. Then the ion-ion repulsion was recalculated based on the positions of the ions at the end of the time step. Finally the trajectory was recalculated using the logarithmic mean of the repulsive force at the beginning and end of the time step, and this final trajectory was kept. The expression for the logarithmic mean is:

$$\log \text{mean } \{a, b\} = (a - b)/\ln (a/b).$$

The logarithmic mean was used in preference to the arithmetic mean to deal in a better way with the situation where the initial ion motion brought the ions very close together. In that instance the force occasionally got very large and the arithmetic mean gave very large jumps where the ions flew apart. This nonphysical result could have been prevented by taking much smaller time steps, but that would have dramatically increased the computer time necessary for the calculations. The algorithm used for the ion-ion repulsions was validated by doing simulations in which two and three ions were placed in the channels and the ends of the channel were made reflecting rather than absorbing boundaries. In this instance the statistical distribution of the ions within the channel is an equilibrium situation that can be calculated analytically. The distribution calculated by the Brownian dynamics simulation was found to agree well with the analytically calculated equilibrium distribution. Since the Coulomb repulsive force between the ions in our model formulation becomes singular as the ions come very close together, the ions in principle should never pass each other. For a few of the simulations in this paper, the ion trajectories were monitored to see whether in fact the ions ever did pass each other. No ion-ion passings were seen. Note that the fact that ions can get closer to, or farther from, each other in the channel implies that ions and water molecules can pass each other in the channel lumen. This is in contrast to the "shaking stack" model of Schumaker (1992) which assumes obligatory single-filing of water molecules and ions. There seems to be at this time no firm evidence favoring one or the other assumption about this aspect of K channel function.

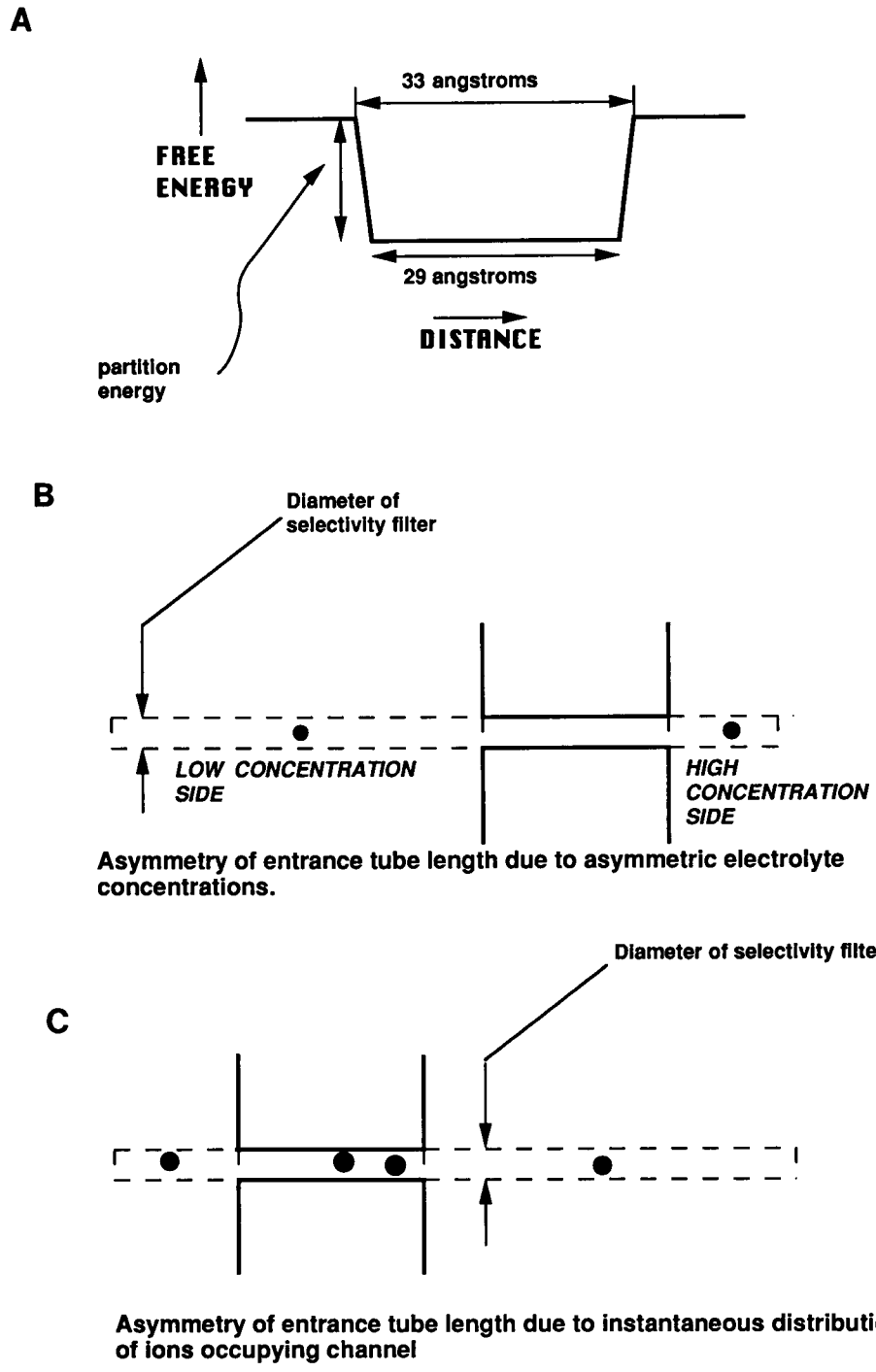

FIGURE 1 (*A*) Schematic representation of partition energy for determining the distribution of ions in the channel. The physical basis for the partition energy is the ability of the channel relative to bulk electrolyte to efficiently "solvate" the ion. The partition energy is the free energy change when the ion trades its bulk solvation environment for a channel hydration environment. (*B*) Schematic representation for how the "entrance tube" length varies with bulk concentration. This is same as previously presented by Cooper et al. (1985). (*C*) Schematic representation for how the "entrance tube" length varies with electrostatic influence from ions already in the channel. Length is proportional to $e^{E/kT}$, where E is the electrostatic energy at the channel mouth for an ion at the mouth interacting with ions in the channel at the time of attempted entry. This variable length feature is new in this paper.

The means of entering the channel was by the "entrance tube" algorithm (Cooper et al., 1985; Jakobsson and Chiu, 1987). In this algorithm, one constructs an imaginary extension of the channel at each end just long enough to contain on the average one ion, at the permeant ion concentration that pertains in the bath at that end. Fig. 1 *B* and *C* illustrate the entrance tube concept. It is seen that the entrance tube is longer if the solution is dilute (*B*) or if there are ions in the channel (*C*). To take account of ions already in the channel, the effective concentration at the channel mouth for calculating the length of the entrance tube is modified by the Boltzmann factor associated with the field due to the ions in the channel. Thus the entrance probability goes down if the channel is already occupied, and it goes down more if the occupying ions are near the channel mouth at which the entrance is being simulated. The physical assumption is that the ionic distribution near the channel mouth is equilibrated with the distribution in the channel itself. This is not precisely true, but is employed as a useful simplifying approximation.

After the entrance tube length is calculated according to the above criteria, an ion is placed in the entrance tube at a random position. Then the ion in the entrance tube is given

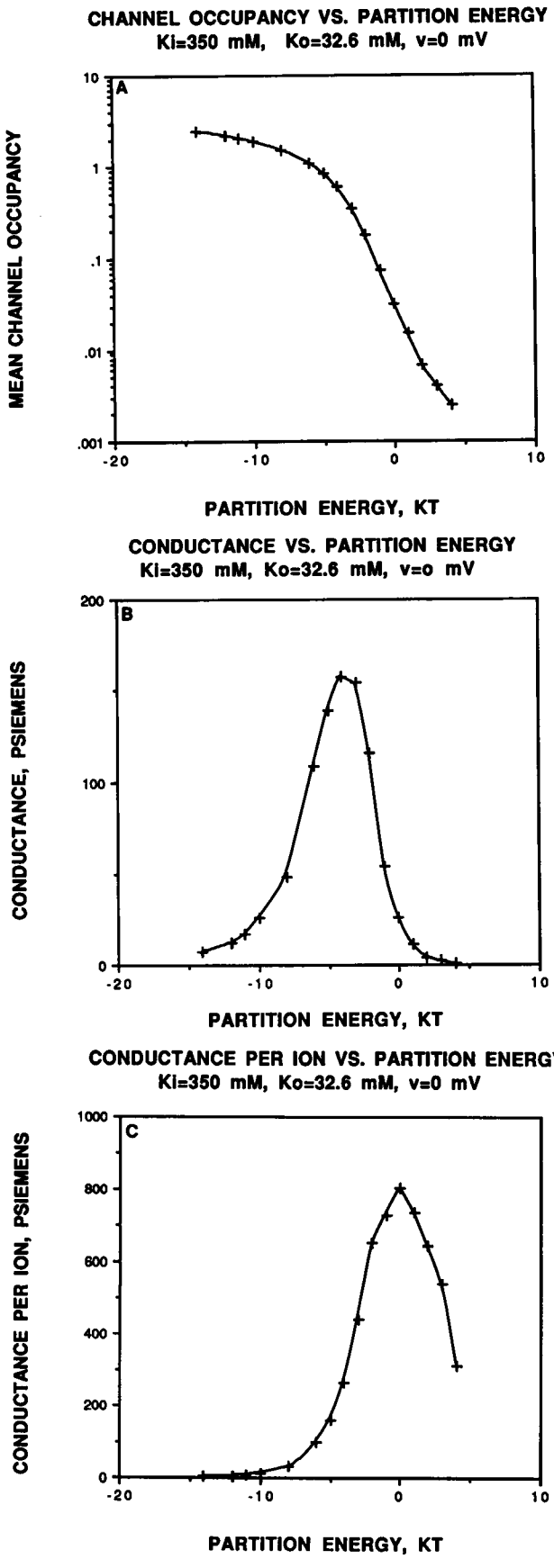

a random jump. If the jump carries the ion into the channel, it continues to move in subsequent time steps according to random jumps, repulsive forces from other ions, the applied field across the membrane and (if it is close to the channel mouth) the free energy gradient associated with making the transition between the bulk and the channel environment. When the ion finally leaves the channel its statistics are added in to other ion trajectories for the length of time in the channel and for the number of ions either translocating the channel or backing out the way they came, whichever is appropriate.

The channel length was 33 Å. This is the length of an α-helix 21 residues long, which is a common membrane-spanning motif in membrane proteins. These parameter choices should not be taken to imply than we believe that the pore of the channel is actually formed by a bundle of membrane-spanning α-helices. It generally is considered to be formed by a linker between two helices (See, for example, Durell and Guy, 1992. On the other hand, for a suggestion that channel pores really are lined by α-helices, see Grove et al., 1991). Whatever the actual structure, the membrane-spanning helix is a convenient guide to defining a reasonable length to assume for a channel pore. The cross-sectional area at the channel mouth is 8.6 $Å^2$, which is a commonly cited size for the selectivity filter in K channels (Hille, 1975; Dwyer et al., 1980). Note that the only place in which the cross-sectional area enters into the calculations is in calculating the ion entry probability. Thus the model parameters do not address the question of the cross-sectional area deep in the channel. The fact that the ions can move closer to each other or farther apart during the course of the simulation implies that ions can pass by water molecules within the channel. However, ions do not pass each other, because the ion-ion repulsive forces become too large as the ions approach the same position in the channel. Simulations for Figs. 2 and 5 were run 20,000,000 time steps (a simulation of 20 μs), while simulations for Figs. 3 and 4 were 200,000,000 time steps (200 μs). The computations were done on Silicon Graphics workstations in the local network of the Compu-

FIGURE 2 (*A*) Mean channel occupancy vs. partition energy for physiological potassium concentrations (350 mM intracellular and 32.6 mM extracellular) and a transmembrane potential of 0 mV. At very low occupancy the occupancy rate goes up exponentially with a reduction in partition energy, but saturation effects appear when significant levels of multiple occupancy begin to occur. (*B*) Single channel conductance under the same conditions as *A*. At low occupancy the conductance goes up with declining partition energy as more charge carriers are available for carrying current. However, at large negative partition energy the conductance falls with declining partition energy as ions become trapped in the channel. The peak conductance is at a partition energy of −4 kT and is a bit over 150 pS, in reasonable correspondence to the maximum single channel conductance seen in K channels. (*C*) Single channel conductance divided by mean channel occupancy (values in *B* divided by the values in *A*) vs. partition energy. This ratio is a measure of how easy it is for each ion to cross the channel. This curve peaks at a partition energy of 0, suggesting that the easiest way for an ion to cross the channel is the situation in which there is neither a potential barrier or a well. This agrees with the general result that diffusion is most rapid across a smooth rather than a rough potential profile (Zwanzig, 1988).

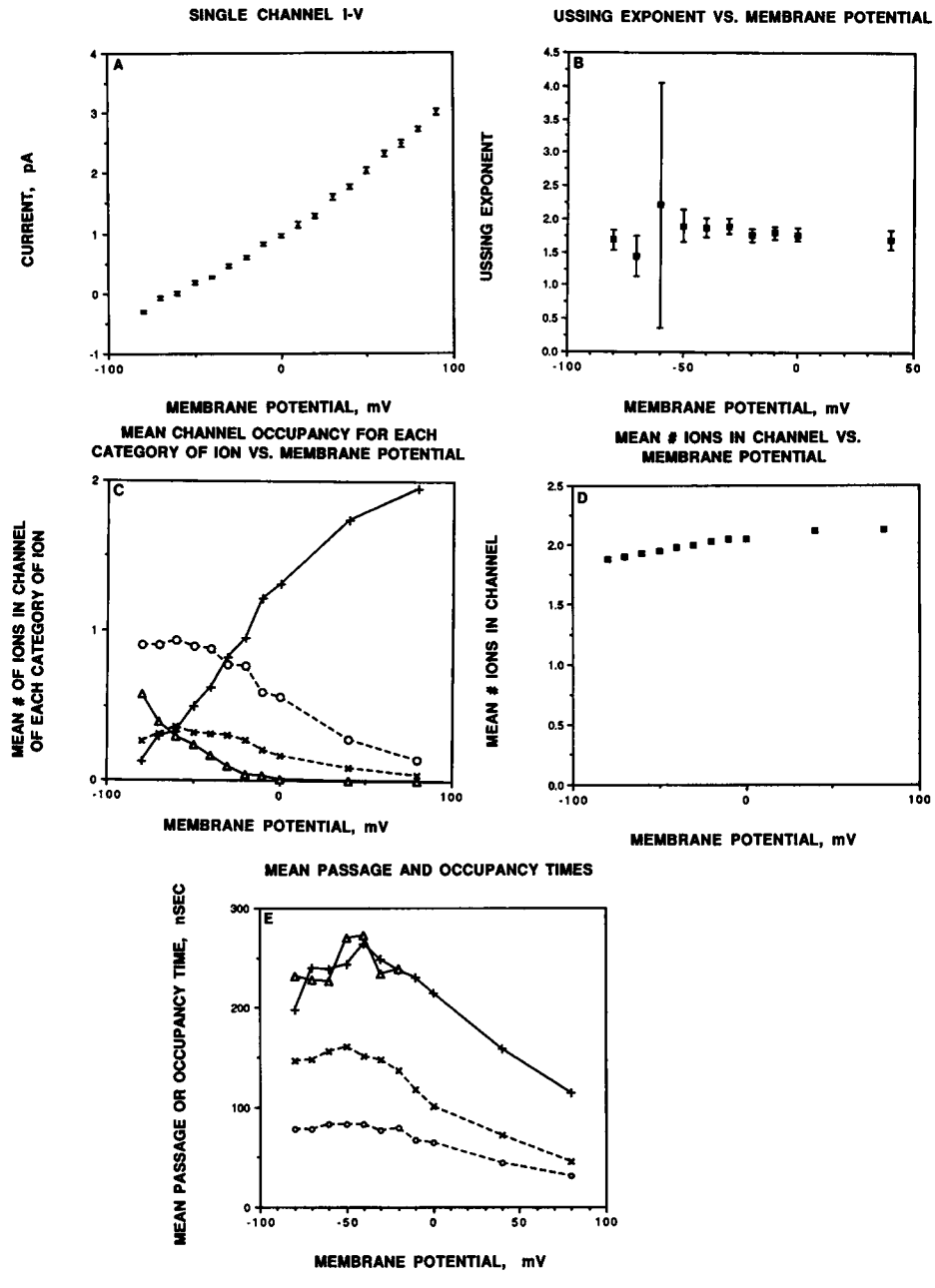

FIGURE 3 (*A*) Single channel current-voltage curve for −11 kT partition energy, 350 mM intracellular and 32.6 mM extracellular concentrations. Error bars according to the "square-root-of-*n*" rule. The figure shows that ion-ion interactions in the channel produce an essentially linear I-V relationship, even with asymmetric concentrations. Conductance is of appropriate magnitude for squid axon K channels (Conti et al., 1975; Llano et al., 1988). (*B*) Ussing flux ratio exponent for those simulations in *A* where ions were observed passing through the channel in both directions, thus making the exponent possible to compute. Error bars are by the square root of the dispersion applied to each unidirectional flux. Results are consistent with experimental results on squid axon K channels in that the Ussing flux ratio exponent is always clearly >1 (Hodgkin and Keynes, 1955), but the voltage dependence of the exponent seen experimentally by Begenisch and De Weer (1980) is not seen in the simulations. (*C*) Mean number of ions in the channel as a function of voltage for the simulations of *A*. There is a close correspondence seen between the Ussing flux ratio exponent in *B* and the mean number in the channel at the same voltage in this figure. (*D*) Mean number of each class of ion that occupies the channel, same simulations as *A*. +, ions that enter from the high concentration side and leave the low concentration side; ○, ions that enter from the high concentration side and leave the same way; △, ions that enter from the low concentration side and leave from the high concentration side; ×, ions that enter from the low concentration side and leave from the same side. (*E*) Mean times for individual ions to occupy the channel in each of the four categories as *D*.

tational Biology Group of the University of Illinois/National Center for Supercomputing Applications.

To test the robustness of the results, or how sensitive they are to choice of parameters, some of the simulations were done with other parameter choices. A full set of simulations were done with the cross-sectional area for ion capture set at twice the value given above. Some simulations were done with dielectric constants of 5 and 40 as well as 20, with diffusion coefficients of 1/2 and 1/5 of the bulk value for potassium as well as for the bulk value, and with several different combinations of diffusion coefficient and dielectric constant. In addition, some simulations were done with shorter channels, 17 Å rather than 33. The robustness with respect to parameter variation of the results presented in this paper will be considered in the Discussion and Summary section of this paper.

RESULTS

Fig. 2 shows the main effects of the partition energy at the mouth of the the channel. This figure shows the results of computations with unbalanced electrolyte concentrations typical of trans-plasma membrane potassium in marine invertebrates such as the squid (350 mM inside, 32.6 mM outside), and transmembrane potential of 0 volts. Fig. 2 *A* shows that the mean occupancy of the channel increases monotonically as the partition energy becomes more favorable (i.e., negative) as expected. However, the increase is much

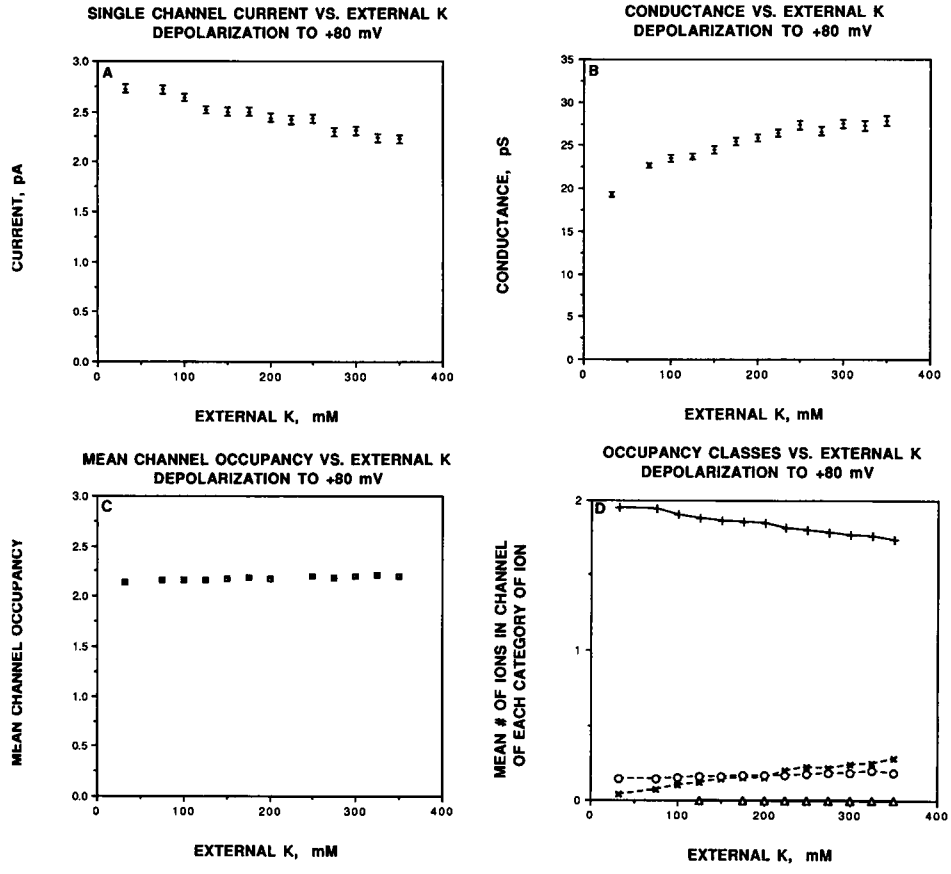

FIGURE 4 (*A*) Single channel current vs. external concentration, internal concentration is 350 mM, partition energy is −11 kT, membrane potential is +80 mV. Error bars calculated by the "square-root-of-*n*" rule. Decline in current resembles that due to extracellular potassium accumulation seen in intact squid axons during extended depolarizing voltage clamp (Frankenhaeuser and Hodgkin, 1956). (*B*) Single channel conductance for same computations as *A*. Error bars calculated by the "square-root-of-*n*" rule. It is seen that although the current declines with increasing $[K]_o$, the conductance increases. (*C*) Mean channel occupancy for the same computations as *A* and *B*. It is seen that the mean channel occupancy increases slightly and approximately linearly with increasing $[K]_o$. (*D*) Average number ions of each category, for the same simulations as *A*, *B*, and *C*. +, ions that enter from the intracellular side and leave the extracellular side; ○, ions that enter from the intracellular side and leave the same side; △, ions that enter from the extracellular side and leave the intracellular side; ×, ions that enter from the extracellular side and leave the same side.

less than would be predicted from a simple application of a Boltzmann relationship, considering only the partition energy for each individual ion between the channel and the bulk. The reason for the discrepancy is that the ion-ion interaction energy within the channel is substantial, so it is much harder for the second ion to enter the channel than the first, harder for the third than the second, and so on. Fig. 2 *B* shows that the conductance is a biphasic function of the partition energy, achieving its maximum value of more than 200 pS at a partition energy of −4 kT. Fig. 2 *C* gives another perspective on these results by showing the conductance/mean channel occupancy for the same runs as 2 *A* and 2 *B*. Conductance divided by concentration should be directly proportional to mean mobility for the individual ions for translocating the channel. Fig. 2 *C* shows that this quantity is maximized at 0 partition energy. When the partition energy is made more negative, the effective mobility for translocation is reduced because it is harder for the ions to leave the channel. When the partition energy is made more positive, the effective mobility for translocation is reduced because it is harder for ions to enter the channel; i.e., there is a barrier for translocation. The results shown in Fig. 2 *C* are an extension of a principle that has long been known to pertain to a single diffusing particle. This is that a smooth potential profile gives the maximum diffusion coefficient. Roughening the potential profile reduces the mobility (Zwanzig, 1988; Lifson and Jackson, 1962; Jakobsson and Chiu, 1988). In Fig. 2 *C* we see the extension of this principle to a situation of multiple mutually interacting particles. In comparing *A*, *B*, and *C*, it is seen that the biphasic behavior of the conductance (*B*) is seen to arise from two counterbalancing tendencies. As the partition energy becomes more negative, the conductance tends to increase from more ions being in the channel available to carry current, but the conductance tends to decrease from it being more difficult for each ion to cross the channel. Thus the conductance is maximized at an intermediate negative partition energy.

It is of interest that the maximum conductance in Fig. 2 *B* is of the same order of magnitude as the maximum single channel conductance seen in potassium-selective channels (Hille, 1992). Thus by adjusting only the one adjustable parameter in our model, the partition energy for potassium ions between the bath and the interior of the channel, the model approximately spans the full range of single channel conductances observed experimentally.

The results of Fig. 2 were used to select the value of the partition energy that makes the model channel behave most like a particular biological K channel, the squid axon delayed rectifier channel. The single channel conductance of this channel has been measured at 12–20 pS (Conti et al., 1975, Llano et al., 1988). Just from this conductance, there might be two values of the partition energy that would be appropriate for this channel, either about +1 kT or −11 kT (negative inside the channel). The decision between these two is

based on occupancy. The Ussing flux ratio exponent for this channel has been found to be 1.5 to 3.3 (Hodgkin and Keynes, 1955; Begenisch and de Weer, 1980). Therefore the channel shows substantial multiple occupancy, so the better choice is clearly the −11 kT energy.

Fig. 3 shows the voltage-dependent properties of the model channel with −11 kT partition energy. Fig. 3 *A* shows the single-channel current-voltage curve, and Fig. 3 *B* and Fig. 3 *C* show the Ussing flux ratio exponent and mean number of ions in the channel as a function of transmembrane voltage.

To calculate the error bars in Fig. 2, the "square-root-of-*n*" rule was used. That is, the fractional error in the current was taken to be $n^{-1/2}$, where n was the net number of ions that crossed the channel in the course of the simulation. From Fig. 3 *A*, it appears that the open single channel current-voltage curve for this channel model is almost linear. There appears to be some systematic curvature to the I-V relationship in Fig. 3 *A*, but it is much less pronounced than the GHK curve associated with a constant field in the membrane and independent ion motions (Goldman, 1943).

To calculate the error bars for the Ussing ratio in Fig. 3 *B*, the error bar for each unidirectional flux was estimated to be the square root of the dispersion (Npq), where N is the total number of ions that entered from one side, p is the probability that those ions emerged from the opposite side from which they entered, and q is $1 - p$; i.e., the probability that those ions emerged from the same side they entered. (For the derivation of the dispersion, see Reif, 1965.) The value of the flux ratio exponent at −60 mV shows a very large error bar. This is because near the equilibrium potential of −62 mV the number of ions moving down the voltage gradient are almost equal in number to those moving in the opposite direction. In this region, the value of the Ussing exponent is very sensitive to small variations in the unidirectional fluxes; right at the reversal potential the expression for the Ussing exponent becomes singular. Hence, very small variations in the unidirectional fluxes in this voltage region will lead to a large fluctuation in the Ussing exponent and large error bars. This could only be overcome by very much longer computer simulations. The fact that the flux ratio exponent is clearly >1 is in agreement with experiments (Hodgkin and Keynes, 1955; Begenisch and De Weer, 1980). However, our simulations do not show the voltage dependence of the flux ratio exponent seen by Begenisch and De Weer.

Fig. 3 *C* shows a slight but clear systematic increase of mean number of ions in the channel with depolarization. The random errors for channel occupancy are somewhat less than for the Ussing exponent. This is because the channel occupancy represents the mean tendencies associated with literally millions of random steps, whereas the Ussing exponent is calculated from a relatively smaller number of discrete events (the traversing of the entire channel by ions). Comparing Fig. 3 *B* and 3 *C*, it is seen that there is a close correspondence between the mean number of ions in the channel and the Ussing flux ratio exponent.

Fig. 3 *D* shows as a function of voltage the mean number of ions occupying the channel of each of the four categories of ions: 1) those that entered the high-concentration (intracellular) side and traversed the channel; 2) those that entered the low-concentration (extracellular) side and traversed the channel; 3) those that entered the high-concentration side and backed out; and 4) those that entered the low-concentration side and backed out. At far depolarized (positive) voltages the channel occupancy is dominated by ions that enter from the high-voltage high-concentration side and moved down their concentration and voltage gradients. Near the equilibrium potential the ions traversing the channel from both directions have occupancies that are about equal. Since these fluxes are also about equal, this implies that the mean passage time for an ion to traverse the channel against the voltage gradient is about the same as the mean passage time for an ion to traverse the channel with the voltage gradient. It was previously shown for the singly-occupied channel that the mean passage time for a permeant ion to cross the channel against the voltage gradient is the same as the mean passage time with the voltage gradient. On the other hand ions that enter from the low concentration side and back out are found in higher concentration than those that enter from the high concentration side and back out. This is because a larger fraction of those that enter from the high concentration side traverse the membrane. Physically this is apparently because, after an ion enters from the high concentration side, a second ion enters from the same side relatively soon and makes it much less likely for the first ion to come back out the same side.

Fig. 3 *E* from the same simulations shows the mean passage times for individual ions that traverse the membrane (*solid lines*) and occupancy times for individual ions that back out of the channel (*dotted lines*). The occupancy time for ions that leave the same side they enter is systematically lower than for ions that traverse the membrane, apparently because the ions that cross the channel have to travel a longer distance than the ions that simply go in and back out. Note that the mean passage times for ions going in both directions are approximately the same at each voltage. This result seems counterintuitive, since one might expect it to take longer for an ion to traverse the membrane against the voltage gradient, as opposed to with the voltage gradient. However, we found in an earlier study on singly-occupied channels, for which an exact numerical solution for mean passage times is obtainable, that the mean passage times for traversing the channel with and against the voltage gradient were exactly the same (Jakobsson and Chiu, 1987). The result in Fig. 3 *E* suggests that a similar phenomenon may pertain for the multiply-occupied channels, for which we do not have an exact solution. Big depolarizing voltages clearly reduce the passage time for ions traversing the membrane, as the channel behavior becomes dominated by ions traversing the membrane down the voltage gradient. At large hyperpolarizing voltages, where the major flux is against the concentration gradient so that the channel is cluttered with ions that do not contribute to the net flux, this effect is much less pronounced. However,

there does seem to be a trend for the passage and occupancy times to become smaller for far hyperpolarized as well as far depolarized voltages.

Fig. 4 shows for the "squid potassium-like" (−11 kT partition energy) channel another behavior similar to what is seen experimentally. Here the intracellular concentration is maintained at 350 mM and the voltage is held at a far depolarization (80 mV), while the extracellular concentration is increased. This emulates the experimental situation in which potassium accumulates in the extracellular or Schwann cell layer during a sustained outward current (Frankenhaeuser and Hodgkin, 1956). From Fig. 4 *A* it is seen that the outward current decreases with increasing extracellular concentration, in agreement with experiment. Fig. 4 *B*, representing the same computations, shows that the simulated conductance, defined as $I_K/(V_K - V)$, increases with extracellular potassium concentration. Comparing *A* with *B*, it is seen that increasing the extracellular concentration causes the current to decrease while simultaneously making the conductance increase. Interestingly, the mean number of ions in the channel increases only very slightly with increasing extracellular ionic concentration (Fig. 4 *C*). Fig. 4 *D* shows the categories of ionic occupancy as a function of extracellular concentration. The vertical axis is the mean number of ions in the channel in each of four categories: 1) entered from the intracellular side and traversed the channel; 2) entered from the extracellular side and traversed the channel; 3) entered from the intracellular side and backed out; and 4) entered from the extracellular side and backed out. It is clear that the majority of channel occupancy is due to ions that traverse the membrane from the intracellular to the extracellular side, and that there is essentially no flux in the opposite direction. By comparing Fig. 4 *D* and 4 *C* it is seen that raising the extracellular concentration in this set of simulated experiments has two effects on ions entering from the intracellular side. It makes it harder for them to cross the channel and causes them to be partly displaced by ions entering from the extracellular side. But it does not cause a significant increase in total channel ionic occupancy.

Experiments have been done in which symmetric concentrations of various magnitude have been placed on both sides of squid axon K channels (Wagoner and Oxford, 1987). Fig. 5 shows simulations of this situation, for a large depolarization to 80 mV, for our "squid-like" K channel. Fig. 5, *A* to *C*, show the conductance, occupancy, and conductance/occupancy respectively of this channel as a function of potassium concentration. From these figures the channel shows some saturating behavior, since the curves are markedly sublinear at high concentrations. A different picture of what is happening is seen in Fig. 5 *D*, where the conductance/occupancy ratio is plotted against the mean channel occupancy. Fig. 5 *D* shows clearly that, where the partition energy is constant and the concentrations are symmetrical, increasing channel occupancy makes it easier for individual ions to

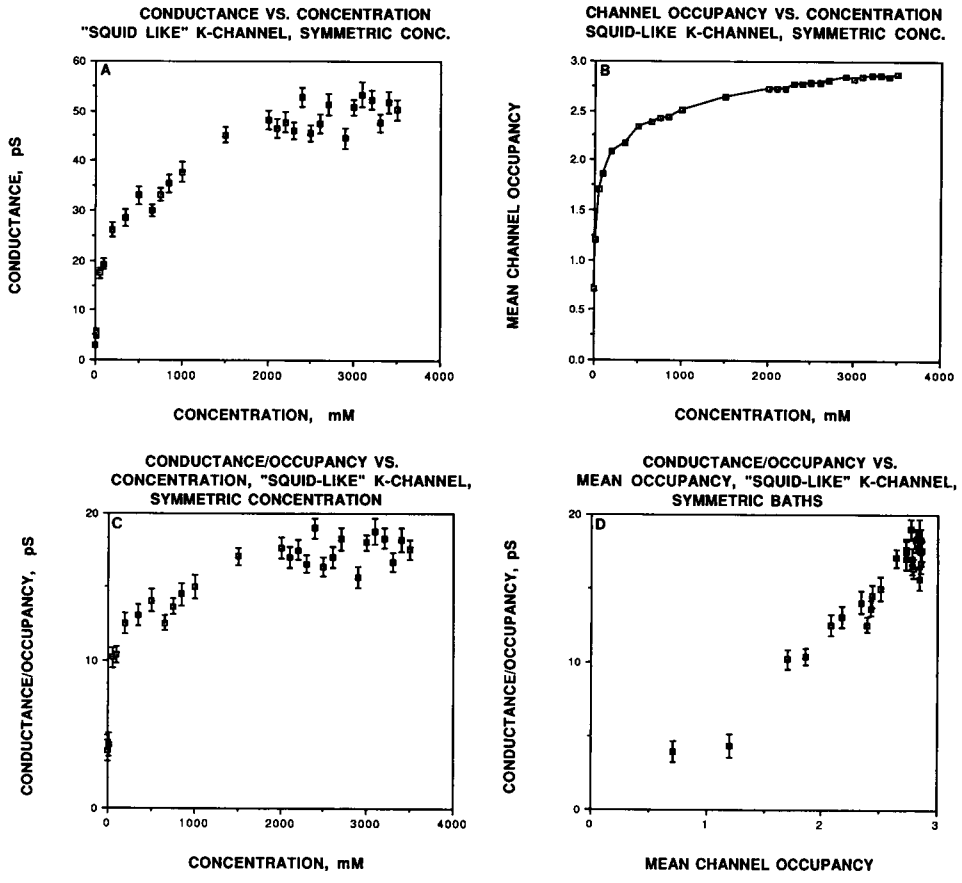

FIGURE 5 Simulations on the "squid-like" channel (−11 kT partition energy) with symmetric electrolyte concentrations. Error bars for *A*, *C*, and *D* calculated by the "square-root-of-*n*" rule. (*A*) Single channel conductance vs. concentration, showing a sharp rate of rise at low concentrations and lower rate of rise at high concentrations. (*B*) Channel occupancy vs. concentration, showing a similar pattern as conductance. (*C*) Conductance/occupancy (a measure of ease with which individual ions cross the channel) vs. concentration. A similar pattern to conductance and occupancy is shown. (*D*) Conductance/occupancy vs. occupancy. This curve shows no sign of saturation, indicating that the more ions in the channel, the easier it is for each ion to pass through the channel. Ion-ion repulsion helps ions overcome the energy barrier for exiting the channel (Fig. 1).

cross the membrane. The conductance/occupancy appears ready to increase without limit as a function of occupancy, at least for physically reasonable concentrations. Presumably this is because ion-ion repulsion in the channel makes it easier for ions in the channel to leave up the partition energy "hill." An analogous effect can be seen in Eyring-type models (von Kitzing, 1992). The sum total of the curves of Fig. 5 show that whatever saturation the channel shows is due to saturation in the occupancy, while the effective mobility of individual ions rises steadily with occupancy. Our results show no sign of the supersaturation effect seen experimentally by Wagoner and Oxford (1987), in which the conductance decreases with increasing potassium ion concentration. Therefore something significant has been omitted from our model that is present in the actual delayed rectifier K channel. This will be discussed below.

DISCUSSION AND SUMMARY

This paper describes a relatively simple Brownian dynamics representation of ions interacting via Coulomb interactions in a simulated pore. While neglecting much of the complexity associated with a detailed with a detailed channel structure, this model replicates much of the behavior of open K channels. These behaviors include reasonable current-voltage curves, saturation, Ussing flux ratio exponents comparable to experiment, and the effects of potassium accumulation in extracellular spaces. The model has no preferred binding sites for ions. Therefore these results prove that there is no need to invoke preferred binding sites in the channel to explain these experimental phenomena. Rather they can arise from the mutually repulsive interactions among cations diffusing in a selective channel. Thus one cannot infer from saturation and apparent binding behavior seen electrophysiologically whether the microscopic physics of ion permeation in a multiply-occupied channel is diffusive or Eyring-like. Rather an explicit physical model of the channel must be constructed to answer this question (Chiu et al., 1993).

The parameters in the simulations are derived directly from reasonable physics for the channel. On the other hand there is a range of reasonable parameter values for many of these parameters. Therefore in addition to the calculations whose results we present in detail we did calculations with various values of dielectric constant, channel length, permeant ion diffusion coefficient, and cross-sectional area for ion entry. In particular we did calculations with dielectric constants of 5 and 40 as well as 20, with diffusion coefficients of 1/2 and 1/5 of the bulk value as well as for the bulk value, with the cross-sectional area of the channel mouth increased by a factor of two, and with a channel length of 17 Å as well as 33 Å. The main features of the model behavior were robust. In all cases as the partition energy was varied the peak conductance was seen at a partition energy of −3 to −4 kT, as in Fig. 2 *B*. In all cases the conductance per ion in the channel peaked at a partition energy of 0 kT. The general saturation properties of the channel were similar, with some relatively minor quantitative differences. The most striking difference from the parameter variations was in the magnitude of the conductances. When the diffusion coefficient was varied the conductance was always found to be simply directly proportional to the diffusion coefficient. For the one variation of channel length that we made, the conductance per ion in the channel was much greater for the shorter channel, but the occupancy was somewhat less for the same bath concentration and partition energy. The net result of the two opposing effects was to make conductance approximately inversely proportional to the channel length. Increasing the dielectric constant in the channel increased the conductance and reducing the dielectric constant reduced it, but the effects were not especially dramatic. Raising the dielectric constant from 20 to 40 increased the peak conductance at −4 kT partition energy by about 1/5; reducing the dielectric constant from 20 to 5 reduced the peak conductance by about 1/5. Increasing the channel mouth cross-sectional area by a factor of two shifts the saturation curves somewhat but leaves the overall qualitative behavior of the model unchanged. This change in channel mouth area is exactly equivalent in the model to increasing the bulk concentration by a factor of two. At low concentrations this increases current by nearly a factor of two. But in conditions where there is multiple occupancy of the channel, which are the most significant for the the normal physiology of many K channels, the effect is relatively minor. Parameter variation in the model should be considered in the context that there are variations in the reported experimental behavior of K channels, even when the experiments are done on the same species and type of channel. For example, Hodgkin and Huxley (1952) originally reported that the instantaneous I-V curve for squid axon delayed rectifier K channels was linear under physiological concentrations. Some subsequent workers have continued to observe that these I-V curves do not deviate substantially from linearity (J. W. Moore, personal communication). On the other hand Clay (1991) has reported that the instantaneous I-V curve for these channels displays the same degree of curvature as the constant-field GHK equation. Similarly Wagoner and Oxford (1987) reported substantial sublinearity in the conductance vs. concentration curves for these channels with symmetric K concentrations below 500 mM. On the other hand Clay (1991) reported that the conductance was linearly proportional to the concentration for these same channels up to a symmetrical concentration of 500 mM. The differences in experimental technique and conditions that account for these different behaviors are not known. Because of such differences, it does not seem useful to fit our model parameters very precisely to any particular data, but rather to vary the parameters to explore the types of behaviors that the model exhibits.

The one adjustable parameter in the model that cannot be derived even approximately in a simple way is the partition energy for ions to enter the channel from the bath. This parameter can only be derived by free energy computations with a microscopically correct molecular structure for the channel. Future plans in our laboratory include doing such calculations using proposed K channel structures such as

those of Durell and Guy (1992) or Bogusz and Busath (1992). For the purposes of the present study, we varied this partition energy over a wide range of values and explored the consequences for channel permeation properties. Varying the partition energy while leaving all other parameters unchanged produces the full range of conductances that are seen in K channels experimentally. This result suggests that the partition energy may be a prime basis for variability among different species of K channels.

An interesting result of the computations is that increasing the occupancy of ions in the channel may result in either increased or decreased conductance and current. This depends on whether the occupancy is increased by making the partition energy more negative or by increasing the bath concentration. Increasing the occupancy by making the partition energy more negative has a dual effect on conductance. Up to a point, making the partition energy more negative increases the conductance by increasing the density of current carriers in the channel. Past that point, the increase in the number of current carriers is more than balanced by the tendency of the current carriers to be trapped in the channel. This dualism is shown in Fig. 2 *B*. If the bath concentration is the same on both sides of the membrane and is increased, the occupancy (Fig. 5 *B*) and conductance (Fig. 5 *A*) both increase. In this case not only does the number of current carriers increase (Fig. 5 *B*), but the individual ions get across the ions more readily (Fig. 5 *D*), due to some ions being pushed out of the channel by others. If the bath concentration is asymmetrical and is increased on the low-concentration, low-voltage side of the membrane, the occupancy (Fig. 4 *C*) and the conductance (Fig. 4 *B*) are essentially unchanged, while the current is reduced (Fig. 4 *A*). All of these behaviors are similar to what is seen experimentally, suggesting that this simple, relatively non-detailed model may capture a lot of the essence of the behavior of the K channel.

On the other hand, the model does not replicate the voltage-dependence of the Ussing flux ratio exponent seen by Begenisch and De Weer (1980). Another experimental behavior that the channel model in this paper does not replicate is the particular type of "supersaturation" reported by Wagoner and Oxford (1987), in which the membrane conductance in symmetrical solutions of permeant ion can actually decline with increasing permeant ion concentration. One possible explanation for this behavior is that the mobility of ions in the channel may be a function of ionic occupancy. Molecular dynamic simulations on the gramicidin channel suggest that channel flexibility enhances permeability (Chiu et al., 1991). It may be that occupancy of the channel by potassium ions stabilizes the pore region of the channel into a more rigid structure, thus reducing the diffusion coefficient of the ions in the channel during high occupancy. This effect would tend to reduce the channel conductance at high concentrations of permeant ions, as seen in the Wagoner-Oxford experimental results. The test of whether this explanation is correct will be to determine diffusion coefficients by fluctuation analysis of molecular dynamics simulations of multiply-occupied explicit models of K channels. Also, once we are dealing with explicit molecular models of K channels, it will be appropriate to calculate the ion-ion forces from electrostatics calculations including the detailed channel structure (Holst et al., 1993). These simulations are planned for the future.

The simulations with the reflecting-end channel to validate the accuracy of the ion-ion interaction algorithm were done by Wendy Lee.

This work was supported by the National Institutes of Health, the National Science Foundation, and the National Center for Supercomputing Applications. Parts of it were presented in a poster at the Biophysical Society meetings of 1993.

REFERENCES

Begenisch, T. B., and P. De Weer. 1980. Potassium flux ratio in voltage-clamped squid giant axons. *J. Gen. Physiol.* 76:83–98.

Bogusz, S., and D. Busath. 1992. Is a β-barrel model of the K^+ channel energetically feasible? *Biophys. J.* 62:19–21.

Chen, D., and R. Eisenberg. 1993. Charges, currents, and potentials in ionic channels of one conformation. *Biophys. J.* 64:1405–1421.

Chiu, S.-W., Jakobsson, E., Subramaniam, S., and J. A. McCammon. 1991. Time-correlation analysis of simulated water motion in flexible and rigid gramicidin channels. *Biophys. J.* 60:273–285.

Chiu, S.-W., Novotny, J. A., and E. Jakobsson. 1993. The nature of ion and water barrier crossings in a simulated ion channel. *Biophys. J.* 64:98–108.

Clay, J. R. 1991. A paradox concerning ion permeation of the delayed rectifier potassium ion channel in squid giant axons. *J. Physiol. (Lond.)* 444:499–511.

Conti, F., DeFelice, L. J., and E. Wanke. 1975. Potassium and sodium ion current noise in the membrane of the squid giant axon. *J. Physiol. (Lond.)* 248:45–82.

Cooper, K., Jakobsson, E., and P. Wolynes. 1985. The theory of ion transport through membrane channels. *Prog. Biophys. Mol. Biol.* 46:51–96.

Davis, M. E., Madura, J. D., Luty, B. A., and J. A. McCammon. 1991. Electrostatics and diffusion of molecules in solution. Simulations with the University of Houston Brownian dynamics program. *Computer Phys. Comm.* 62:187–197.

deLevie, R., Seidah, N. G., and H. Moreira. 1972. Transport of ions of one kind through thin membranes. II. Nonequilibrium steady-state behavior. *J. Membr. Biol.* 10:171.

Durell, S. R., and H. R. Guy. 1992. Atomic scale structure and functional models of voltage-gated potassium channels. *Biophys. J.* 62:238–250.

Dwyer, T. M., Adams, D. J., and B. Hille. 1980. The permeability of the endplate channel to organic cations in frog muscle. *J. Gen. Physiol.* 75: 469–492.

Einstein, A. E. 1926. Investigations on the Theory of the Brownian Movement. Dover Publications, New York.

Frankenhaeuser, B., and A. L. Hodgkin. 1956. The after-effects of impulses in the giant nerve fibres of Loligo. *J. Physiol. (Lond.)* 131:341–376.

Goldman, D. E. 1943. Potential, impedance, and rectification in membranes. *J. Gen. Physiol.* 27:37–60.

Grove, A., Tomichi, J. M., and M. Montal. 1991. A molecular blueprint for the pore-forming structure of voltage-gated calcium channels. *Proc. Natl. Acad. Sci. USA.* 88:6418–6422.

Hille, B. 1975. Ionic selectivity of Na and K channels of nerve membranes. *In* Membranes—A Series of Advances, Vol. 3: Lipid Bilayers and Biological Membranes: Dynamics Properties. G. Eisenman, editor. Marcel Dekker, New York. 255–323.

Hille, B. 1992. Ionic Channels of Excitable Membranes. 2nd ed. Sinauer Associates, Sunderland, MA.

Hille, B., and W. Schwarz. 1978. K channels in excitable cells as multi-ion pores. *J. Gen. Physiol.* 72:409–442.

Hodgkin, A. L., and A. F. Huxley. 1952. A quantitative description of membrane current and its application to conduction and excitation in nerve. *J. Physiol. (Lond.)* 117:500–544.

Hodgkin, A. L., and R. D. Keynes. 1955. The potassium permeability of a

giant nerve fibre. *J. Physiol. (Lond.)* 128:61–88.

Holst, M., Kozack, R. E., Saied, F., and S. Subramaniam. 1993. Treatment of electrostatic effects in proteins: multigrid-based Newton iterative method for solution of the full nonlinear Poisson-Boltzmann equation. *Proteins.* In press.

Jakobsson, E., and S.-W. Chiu. 1987. Stochastic theory of ion movement of ion movement in channels with single-ion occupancy. Application to sodium permeation of gramicidin channels. *Biophys. J.* 52:33–46.

Jakobsson, E., and S.-W. Chiu. 1988. Application of Brownian motion theory to the analysis of membrane channel ionic trajectories calculated by molecular dynamics. *Biophys. J.* 54:751–756.

Jordan, P. C. 1982. Electrostatic modeling of ion pores. Energy barriers and electric field profiles. *Biophys. J.* 39:157–164.

Levitt, D. G. 1986. Interpretation of biological flux data: reaction-rate versus continuum theory. *Annu. Rev. Biophys. Biophys. Chem.* 15:29–57.

Levitt, D. G. 1991a. General continuum theory for multiion channels. I. Theory. *Biophys. J.* 52:455–466.

Levitt, D. G. 1991b. General continuum theory for multiion channels. II. Application to acetylcholine channels. *Biophys. J.* 59:278–288.

Lifson, S., and J. L. Jackson. 1962. On the self-diffusion of ions in a polyelectrolyte solution. *J. Chem. Phys.* 36:2410–2414.

Llano, I., Webb, C. K., and F. Bezanilla. 1988. Potassium conductance of the squid giant axon. *J. Gen. Physiol.* 92:179–196.

Pallotta, B. S., and P. K. Wagoner. 1992. The voltage-dependent potassium channel since Hodgkin and Huxley. *Physiol. Rev.* 72:549–567.

Reif, F. 1965. Statistical and Thermal Physics. McGraw-Hill, New York.

Schumaker, M. F. 1992. Shaking stack model of ion conduction through the Ca^{2+}-activated K^+ channel. *Biophys. J.* 63:1032–1044.

von Kitzing, E. 1992. A novel model for saturation of ion conductivity in transmembrane channels. *In* Membrane Proteins: Structures, Interactions and Models. A. Pullman, J. Jortner, and B. Pullman, editors. Kluwer Academic Publishers, The Netherlands. 297–314.

Wagoner, P. K., and G. S. Oxford. 1987. Cation permeation through the voltage-dependent potassium channel in the squid axon. *J. Gen. Physiol.* 90:261–290.

Zwanzig, R. 1988. Diffusion in a rough potential. *Proc. Natl. Acad. Sci. USA.* 85:2029–2030.